

## INFRARED SPECTROSCOPY OF SYMBIOTIC STARS. VII. BINARY ORBIT AND LONG SECONDARY PERIOD VARIABILITY OF CH CYGNI

KENNETH H. HINKLE<sup>1</sup>, FRANCIS C. FEKEL<sup>2,4</sup>, AND RICHARD R. JOYCE<sup>3</sup>

<sup>1</sup> National Optical Astronomy Observatory, P.O. Box 26732, Tucson AZ, USA; [hinkle@noao.edu](mailto:hinkle@noao.edu)

<sup>2</sup> Center of Excellence in Information Systems, Tennessee State University, Nashville TN, USA; [fekel@evans.tsuniv.edu](mailto:fekel@evans.tsuniv.edu)

<sup>3</sup> National Optical Astronomy Observatory, P.O. Box 26732, Tucson AZ, USA; [joyce@noao.edu](mailto:joyce@noao.edu)

Received 2008 August 27; accepted 2008 October 29; published 2009 February 24

### ABSTRACT

High-dispersion spectroscopic observations are used to refine orbital elements for the symbiotic binary CH Cyg. The current radial velocities, added to a previously published 13 year time series of infrared velocities for the M giant in the CH Cyg symbiotic system, more than double the length of the time series to 29 years. The two previously identified velocity periods are confirmed. The long period, revised to  $15.6 \pm 0.1$  yr, is shown to result from a binary orbit with a  $0.7 M_{\odot}$  white dwarf and  $2 M_{\odot}$  M giant. Mass transfer to the white dwarf is responsible for the symbiotic classification. CH Cyg is the longest period S-type symbiotic known. Similarities with the longer period D-type systems are noted. The 2.1 year period is shown to be on Wood's sequence D, which contains stars identified as having long secondary periods (LSP). The cause of the LSP variation in CH Cyg and other stars is unknown. From our review of possible causes, we identify g-mode nonradial pulsation as the leading mechanism for LSP variation in CH Cyg. If g-mode pulsation is the cause of the LSPs, a radiative region is required near the photosphere of pulsating asymptotic giant branch stars.

*Key words:* binaries: symbiotic – infrared: stars – stars: individual (CH Cyg) – stars: late-type – stars: variables: other

### 1. INTRODUCTION

Symbiotic stars are mass-transfer binaries, containing a mass-losing red giant and a mass-accreting companion that is usually a white dwarf. One system is known with a neutron star (Hinkle et al. 2006), and systems containing main sequence stars are possible but have proved elusive to identify. Mass transfer causes the symbiotics to exhibit highly complex light variations and spectra. From their characteristics at infrared wavelengths, Webster & Allen (1975) separate the symbiotics into two subclasses: D for dusty-type and S for stellar-type systems. CH Cyg is the brightest of the S-type symbiotic stars.

The current series of papers is concerned with infrared spectroscopy of the late-type star in each symbiotic system. Because velocities of this component are usually well behaved, we employ these spectra to derive single-lined spectroscopic orbits. The orbital elements provide insight into the period distribution, mass ratios, and orbital dynamics of these interacting systems. These results are ultimately of interest in evaluating the potential for catastrophic demise of the stellar components (Iben 2003).

CH Cyg was the topic of our first paper on the infrared spectroscopy of symbiotic stars (Hinkle et al. 1993, hereafter Paper I). As a result of its brightness and placement in the northern sky, CH Cyg is easily observed. Following the publication of Paper I, we continued to monitor CH Cyg with various spectrographs and now have data spanning a period of nearly three decades. In the intervening 16 years since the publication of Paper I, our knowledge of M-giant variables as well as the CH Cyg system itself has greatly increased. We find, in agreement with many others who have worked on symbiotics (see e.g., Skopal et al. 1996a; Crocker et al. 2002; Sokoloski & Kenyon

2003b) that CH Cyg is the most complex of the symbiotics that we have observed.

Based on velocity variations of the M III star in the CH Cyg system, we concluded in Paper I that the CH Cyg system is triple. Two separate stable velocity variations, a long-period variation of  $\sim 14.5$  years and a short-period variation of  $\sim 2.1$  years, were found and are confirmed and refined in the present paper. In the discussion section of Paper I, we proposed a model for this velocity behavior that placed the symbiotic binary in the 2.1 year orbit. Our model, based on the short-period mass function, had three underpinnings.

1. The absence of any other known S-type symbiotic with a confirmed orbital period longer than five years and a mean period distribution for S-type symbiotic orbits of  $\sim$ two years (Fekel et al. 2007).
2. Stellar pulsation theory showing that the two year velocity variation is too long to be the M-giant fundamental pulsation (Hughes & Wood 1990).
3. Weak evidence at that time that the system had a high inclination.

Because this triple-star model has been controversial and new information has accumulated, we decided to reexamine this conclusion. In the present paper, we review all the evidence and show convincingly that the triple-star model with the white dwarf as a member of the short-period system is *incorrect*. We now conclude instead that the system is a binary with the mass-accreting white dwarf in the long-period orbit.

Nonetheless, points (1) and (2) remain valid and are essential to understand CH Cyg. While the CH Cyg symbiotic system has unique properties, we believe that the most interesting aspect of CH Cyg is the nature of the 2.1 year variation. We show that CH Cyg qualifies as the most intensively investigated variable star with long-secondary period (LSP) light and velocity variations. The existence and uncertain nature of the LSP variations is highlighted by Wood (2007).

<sup>4</sup> Visiting Astronomer, Kitt Peak National Observatory, National Optical Astronomy Observatory, operated by the Association of Universities for Research in Astronomy, Inc., under cooperative agreement with the National Science Foundation.

## 2. OBSERVATIONS AND REDUCTIONS

In 1992, we obtained two spectroscopic observations with the Fourier transform spectrometer (FTS) at the coudé focus of the Kitt Peak National Observatory (KPNO) 4 m telescope (Hall et al. 1978). These observations are a continuation of the series of 71 FTS spectra discussed in detail in Paper I. The two observations were obtained in the  $2\ \mu\text{m}$  region and have a resolving power of  $\sim 60,000$ . Shortly after the two new spectra were obtained, the FTS was decommissioned as a result of budget cuts at KPNO.

From 1995 to 2000, we collected 25 observations with the coudé feed telescope and spectrograph system at KPNO. The detector was an infrared camera, NICMASS, developed at the University of Massachusetts. We obtained a 2 pixel resolving power of 44,000 at a wavelength of  $1.623\ \mu\text{m}$ . A more extensive description of the experimental setup can be found in Joyce et al. (1998) and Fekel et al. (2000). The NICMASS equipment was sent to Mount Stromlo Observatory (MSO; Australia) to continue the symbiotic orbit program in the southern hemisphere. This equipment along with the 1.85 m telescope was destroyed in a devastating bush fire that burned over Mount Stromlo in January 2003.

In 2000, three spectra were also acquired with the Phoenix cryogenic echelle spectrograph at the f/15 Cassegrain focus of either the KPNO 2.1 or 4 m telescopes. A complete description of the spectrograph can be found in Hinkle et al. (1998). The observations were centered at either  $1.563$  or  $2.226\ \mu\text{m}$  and have resolving powers of either 50,000 or 70,000. An expanded discussion of the experimental setup is in Fekel et al. (2000). Phoenix was deployed to the southern hemisphere in 2000.

Finally, five spectrograms were obtained in 2007 and 2008 with the KPNO coudé feed telescope, coudé spectrograph, and a CCD with enhanced red sensitivity, designated LB1A. This  $1980 \times 800$  pixel CCD was manufactured by Lawrence Berkeley National Laboratory and is  $300\ \mu\text{m}$  thick. Although this thickness resulted in increased pixel contamination by cosmic ray and background events, the chip was used because of its high-quantum efficiency at far-red wavelengths. Our spectrograms, centered near  $1.005\ \mu\text{m}$ , have a wavelength range of  $420\ \text{\AA}$  and a resolving power of  $\sim 21,500$ .

Reduction and radial velocity measurement of the FTS spectra are discussed in detail in Paper I. For the NICMASS and Phoenix data standard observing and reduction techniques were used (Joyce 1992). Wavelength calibration at the infrared wavelengths of  $1.563$ ,  $1.623$ , and  $2.226\ \mu\text{m}$  posed a challenge, because the spectral coverage was far too small to include a sufficient number of ThAr emission lines for a dispersion solution. Thus, our approach was to utilize the absorption lines of a K III star. Several sets of lines were tried, including CO, Fe I, and Ti I. These groups all gave consistent results. For the spectrograms acquired with the LB1A CCD at  $1.005\ \mu\text{m}$ , we were able to use ThAr spectra for wavelength calibration. Telluric lines are present in the  $1.005$  and  $2.226\ \mu\text{m}$  wavelength regions. These lines were removed from our observations by ratioing the spectra to a hot-star spectrum observed on the same night.

For all of our spectra except those obtained with the FTS, the absorption line radial velocities of CH Cyg were measured with the IRAF cross-correlation program FXCOR (Fitzpatrick 1993). Those velocities were determined relative to the M-giant International Astronomical Union velocity standards  $\delta$  Oph or  $\alpha$  Cet, which have radial velocities of  $-19.1$  and  $-25.3\ \text{km s}^{-1}$ , respectively (Scarfe et al. 1990). The standards were observed

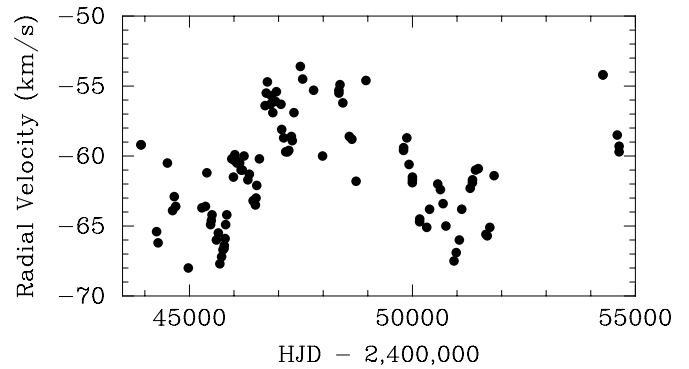


**Figure 1.** Our 106 KPNO radial velocities, derived from lines in the near infrared, of the CH Cyg M-giant component plotted vs. heliocentric Julian day. The data span nearly 30 years. A short period, 2.1 year, and a long period, 15.6 year, variation are apparent.

multiple times during the course of each night. For the FTS spectra, which cover a wavelength range that is  $\sim 100$  times greater than the other spectra, velocities were referenced to telluric lines.

## 3. ORBITAL SOLUTION

Our 106 KPNO observations, which span nearly 30 years, are listed in Table 1, and the velocities are plotted in Figure 1 versus heliocentric Julian date. That plot clearly shows two periodicities. Thus, we have employed the general least squares program of Daniels (1966) to obtain a simultaneous orbital solution for the short- and long-period velocity variations of CH Cyg. All KPNO velocities were given unit weight after a comparison of the FTS velocities with those from the Phoenix and coudé feed spectrographs showed that the rms values of the velocity data sets were nearly identical. We then computed several different orbital solutions. The first used only the KPNO velocities, while, similar to a solution of Paper I, the second included the velocities of Deutsch et al. (1974), Yamashita & Maehara (1979), and Yoo & Yamashita (1991) plus our KPNO velocities and is designated the all-velocity solution. Weights adopted for the non-KPNO velocities are the same as those assigned in Paper I. As was done in that paper, we have also computed orbital solutions with the short-period eccentricity fixed at 0.0. However, given the systematic residuals that result from adopting such a sinusoidal fit and our discussion and conclusion about whether this short-period velocity variation results from orbital motion or pulsation, we do not discuss the  $e = 0.0$  solutions any further.

A comparison of the two remaining solutions shows that the long period of the KPNO-only solution is nearly 40 days longer than that of the all-velocity solution, but that difference is only 0.7% and is less than the period uncertainty. Uncertainties of the orbital parameters in the all-velocity solution are somewhat smaller than those in the KPNO-only solution, as would be expected because of the longer baseline of data, but the parameter values of both solutions are within those uncertainties. Thus, in Table 2, we have chosen to adopt the more homogeneous solution that includes only our KPNO velocities.

For the individual observations, Table 1 lists the heliocentric Julian date, the observed total velocity, and the observed minus calculated velocity residual ( $O - C$ ) to the combined orbit. Also computed and listed in the table are the long-period orbital phase, the long-period velocity, which is equal to the total velocity minus the computed short-period velocity, the short-

**Table 1**  
Radial Velocities of CH Cyg

HJD 2,400,000 +	RV (km s <sup>-1</sup> )	<i>O</i> - <i>C</i> (km s <sup>-1</sup> )	$\phi_L$	$V_L$ (km s <sup>-1</sup> )	$\phi_S$	$V_S$ (km s <sup>-1</sup> )
43,913.138	-59.2	0.07	0.689	-60.49	0.493	1.37
43,917.267	-59.2	0.13	0.690	-60.45	0.499	1.38
44,263.275	-65.4	0.01	0.751	-62.09	0.960	-3.29
44,297.144	-66.2	-1.63	0.757	-63.88	0.005	-3.94
44,507.607	-60.5	0.39	0.794	-62.74	0.286	2.63
44,622.194	-63.9	-1.99	0.814	-65.55	0.439	-0.33
44,660.373	-62.9	-0.52	0.821	-64.22	0.490	0.80
44,692.110	-63.6	-0.79	0.826	-64.60	0.532	0.21
44,974.297	-68.0	-0.03	0.876	-64.60	0.908	-3.44
45,279.621	-63.7	-1.10	0.929	-65.89	0.315	1.09
45,360.478	-63.6	-0.62	0.944	-65.35	0.423	1.12
45,392.184	-61.2	1.99	0.949	-62.69	0.465	3.48
45,475.199	-64.9	-1.00	0.964	-65.53	0.576	-0.37
45,490.162	-64.6	-0.55	0.966	-65.05	0.596	-0.10
45,507.001	-64.2	0.03	0.969	-64.43	0.618	0.26
45,604.862	-66.0	-0.52	0.987	-64.70	0.749	-1.82
45,647.498	-65.5	0.64	0.994	-63.40	0.806	-1.46
45,683.282	-67.7	-1.00	0.000	-64.90	0.853	-3.80
45,721.218	-67.2	-0.07	0.007	-63.83	0.904	-3.45
45,752.156	-66.7	0.36	0.012	-63.26	0.945	-3.07
45,776.080	-66.6	-0.04	0.017	-63.56	0.977	-3.08
45,782.082	-66.4	-0.04	0.018	-63.54	0.985	-2.91
45,799.055	-65.9	-0.24	0.021	-63.66	0.008	-2.48
45,812.076	-64.9	0.13	0.023	-63.23	0.025	-1.54
45,837.034	-64.2	-0.43	0.027	-63.67	0.058	-0.96
45,948.828	-60.2	0.36	0.047	-62.31	0.207	2.47
45,986.495	-61.5	-1.28	0.054	-63.75	0.258	0.97
46,005.414	-60.3	-0.18	0.057	-62.55	0.283	2.06
46,018.341	-59.9	0.17	0.059	-62.12	0.300	2.39
46,044.386	-60.3	-0.29	0.064	-62.44	0.335	1.85
46,064.855	-60.5	-0.51	0.067	-62.54	0.362	1.53
46,107.908	-60.5	-0.48	0.075	-62.27	0.419	1.28
46,125.872	-60.5	-0.44	0.078	-62.13	0.443	1.18
46,157.791	-61.0	-0.85	0.084	-62.35	0.486	0.49
46,186.830	-61.0	-0.73	0.089	-62.06	0.525	0.33
46,223.774	-60.0	0.46	0.095	-60.65	0.574	1.11
46,310.529	-61.7	-0.56	0.111	-61.16	0.690	-1.10
46,344.562	-61.3	0.21	0.117	-60.19	0.735	-0.90
46,426.835	-63.2	-0.60	0.131	-60.53	0.845	-3.27
46,452.877	-63.2	-0.29	0.136	-60.07	0.879	-3.42
46,478.799	-63.5	-0.43	0.140	-60.06	0.914	-3.86
46,492.844	-63.0	0.04	0.143	-59.52	0.933	-3.44
46,509.786	-62.1	0.73	0.146	-58.74	0.955	-2.63
46,569.772	-60.2	0.26	0.156	-58.88	0.035	-1.06
46,696.608	-56.4	0.01	0.178	-58.50	0.204	2.10
46,721.501	-55.5	0.66	0.183	-57.72	0.237	2.88
46,748.537	-54.7	1.31	0.188	-56.95	0.273	3.56
46,818.466	-56.3	-0.38	0.200	-58.32	0.367	1.65
46,838.810	-55.7	0.26	0.203	-57.60	0.394	2.16
46,869.183	-56.9	-0.85	0.209	-58.58	0.434	0.83
46,931.016	-56.1	0.27	0.220	-57.22	0.517	1.39
46,949.766	-55.4	1.10	0.223	-56.32	0.542	2.02
47,053.636	-56.3	1.19	0.241	-55.86	0.680	0.76
47,069.749	-58.1	-0.40	0.244	-57.41	0.702	-1.09
47,113.295	-58.7	-0.38	0.252	-57.25	0.760	-1.83
47,159.503	-59.7	-0.62	0.260	-57.36	0.821	-2.96
47,201.195	-59.7	0.04	0.267	-56.60	0.877	-3.07
47,229.269	-59.6	0.40	0.272	-56.16	0.914	-3.04
47,286.152	-58.6	0.57	0.282	-55.86	0.990	-2.17
47,307.126	-58.9	-0.61	0.286	-57.00	0.018	-2.51
47,344.045	-56.9	-0.35	0.292	-56.67	0.067	-0.58
47,488.413	-53.6	0.24	0.318	-55.85	0.260	2.49
47,540.384	-54.5	-0.63	0.327	-56.66	0.329	1.53
47,783.636	-55.3	0.73	0.370	-55.16	0.653	0.60
47,985.231	-60.0	-0.57	0.405	-56.53	0.922	-4.04

**Table 1**  
(Continued)

HJD 2,400,000 +	RV (km s <sup>-1</sup> )	<i>O</i> - <i>C</i> (km s <sup>-1</sup> )	$\phi_L$	$V_L$ (km s <sup>-1</sup> )	$\phi_S$	$V_S$ (km s <sup>-1</sup> )
48,352.289	-55.5	-0.88	0.470	-57.31	0.412	0.93
48,353.143	-55.3	-0.67	0.470	-57.10	0.413	1.13
48,377.043	-54.9	-0.04	0.474	-56.52	0.445	1.57
48,440.068	-56.2	-0.63	0.485	-57.23	0.529	0.40
48,586.221	-58.6	-0.70	0.511	-57.64	0.723	-1.67
48,644.104	-58.8	0.31	0.521	-56.77	0.801	-1.72
48,736.250	-61.8	-0.99	0.537	-58.33	0.923	-4.46
48,958.250	-54.6	1.26	0.576	-56.77	0.219	3.43
49,802.024	-59.6	-0.26	0.724	-61.71	0.344	1.85
49,803.979	-59.4	-0.04	0.725	-61.50	0.347	2.05
49,874.957	-58.7	1.43	0.737	-60.34	0.442	3.07
49,923.777	-60.6	0.19	0.746	-61.80	0.507	1.38
49,997.740	-61.9	0.05	0.759	-62.26	0.605	0.40
49,999.695	-61.7	0.28	0.759	-62.03	0.608	0.61
50,000.742	-61.5	0.50	0.759	-61.82	0.609	0.82
50,162.046	-64.7	0.67	0.788	-62.32	0.824	-1.71
50,163.043	-64.5	0.90	0.788	-62.10	0.826	-1.50
50,320.682	-65.1	-0.20	0.815	-63.80	0.036	-1.50
50,385.709	-63.8	-1.14	0.827	-64.97	0.123	0.03
50,567.995	-62.0	0.33	0.859	-64.03	0.366	2.36
50,627.951	-62.4	0.48	0.870	-64.01	0.445	2.09
50,687.829	-63.4	0.15	0.880	-64.45	0.525	1.21
50,750.724	-65.0	-0.62	0.891	-65.32	0.609	-0.30
50,932.878	-67.5	0.08	0.923	-64.72	0.852	-2.70
50,981.853	-66.9	1.33	0.932	-63.45	0.917	-2.12
51,051.770	-66.0	0.87	0.944	-63.85	0.011	-1.28
51,106.744	-63.8	0.58	0.954	-64.06	0.084	0.84
51,295.020	-62.3	-0.26	0.987	-64.44	0.335	1.88
51,345.808	-61.9	0.25	0.996	-63.76	0.403	2.10
51,346.857	-61.7	0.45	0.996	-63.55	0.404	2.30
51,415.767	-61.0	1.46	0.008	-62.28	0.496	2.73
51,477.760	-60.9	1.96	0.019	-61.51	0.578	2.56
51,648.009	-65.6	-0.88	0.049	-63.50	0.805	-2.98
51,677.971	-65.7	-0.56	0.054	-63.02	0.845	-3.24
51,736.808	-65.1	0.50	0.064	-61.63	0.924	-2.97
51,831.701	-61.4	0.98	0.081	-60.60	0.050	0.18
54,271.980	-54.2	0.51	0.510	-56.42	0.304	2.73
54,272.956	-54.2	0.51	0.510	-56.41	0.305	2.73
54,592.984	-58.5	0.42	0.566	-57.43	0.732	-0.65
54,634.970	-59.7	0.13	0.574	-57.86	0.788	-1.71
54,635.982	-59.3	0.55	0.574	-57.44	0.789	-1.31

**Table 2**  
Orbital Elements and Related Parameters of CH Cyg

Parameter	Short-Period Orbit	Long-Period Orbit
<i>P</i> (days)	750.1 ± 1.3	5689.2 ± 47.0
<i>P</i> (years)	2.0537 ± 0.0036	15.58 ± 0.13
<i>T</i> (HJD)	2, 447, 293.5 ± 12.9	2, 445, 681 ± 192
$\gamma$ (km s <sup>-1</sup> )	...	-59.91 ± 0.09
<i>K</i> (km s <sup>-1</sup> )	2.87 ± 0.13	4.45 ± 0.12
<i>e</i>	0.330 ± 0.041	0.122 ± 0.024
$\omega$ (deg)	229.5 ± 7.7	216.9 ± 12.7
<i>a</i> sin <i>i</i> (10 <sup>6</sup> km)	27.90 ± 12.30	345.69 ± 9.09
<i>f</i> ( <i>m</i> ) ( <i>M</i> <sub>⊙</sub> )	0.0015 ± 0.0002	0.051 ± 0.004

period orbital phase, and finally, the short-period velocity, which is equal to the total velocity minus the computed long-period velocity. Figure 2 presents the computed velocity curve of the long-period orbit, compared with the KPNO radial velocities, where zero phase is a time of periastron. Each plotted velocity

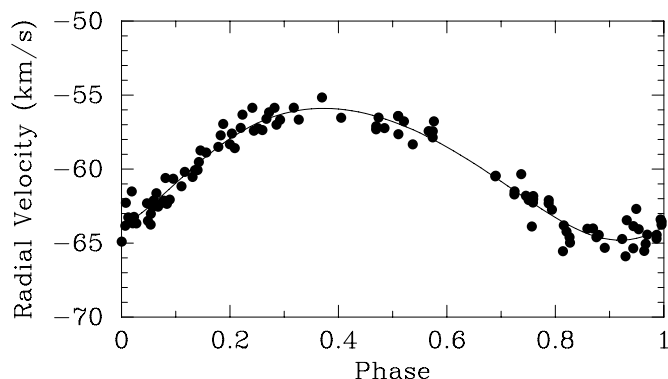


**Figure 2.** The computed velocity curve of the 15.6 yr long period orbit compared with the KPNO radial velocities. Each plotted velocity consists of the total observed velocity minus its calculated short-period velocity. Zero phase is a time of periastron.

consists of the total observed velocity minus its calculated short-period velocity. Figure 3 shows the computed velocity curve of the short-period orbit, compared with the KPNO radial velocities, where zero phase is a time of periastron. Each plotted velocity consists of the total observed velocity minus its calculated long-period velocity.

The radial velocity residuals, listed in Column 3 of Table 1 ( $O - C$ ), were analyzed for possible additional periods. The program PeriodoGRAM (PGRAM) was employed to fit sinusoids to the phased data for periods between 50 and 500 days in steps of 0.05 days. This period finding program works well even for nonsinusoidal curves, with eccentricities as large as  $\sim 0.4$ . Various subsets of data were searched in an attempt to remove false periods. Two possible periods of  $\sim 62$  and  $\sim 170$  days appear in the velocity residuals. However, the velocity semiamplitudes are very small, at maximum  $0.4 \text{ km s}^{-1}$ . Of particular interest, we find no period above the noise in the 90–110 day period range, which corresponds to a photometric period of CH Cyg.

Yamashita & Maehara (1979) first proposed an orbit for the M giant. Despite the use of very heterogeneous data with large uncertainties, they determined a probable period of 5750 days, very close to our value of 5689 days. Although their semiamplitude and eccentricity are rather different from ours, other elements are similar. We also compare our orbital solution to those in Paper I. In that earlier analysis, the long period for the all-velocity solution was 5298 days, while that for the KPNO velocities alone was 5483 days. Thus, the improved period of our adopted solution (Table 2) is nearly 400 days longer than the all-velocity solution in Paper I and about 200 days longer than the KPNO-only solution given in that paper. Comparing other elements of our adopted solution and the KPNO-only solution of Paper I, the orbital elements are similar, but the uncertainties of the long-period elements have been significantly reduced.

The ephemeris for conjunctions with the M giant in front of the white dwarf, which corresponds to times of mideclipse, is

$$T_{\text{conj}}(\text{HJD}) = 2,446,353(\pm 192) + 5689(\pm 47)E, \quad (1)$$

where  $E$  is an integer number of cycles. The above ephemeris for the eclipse of the white dwarf by the M giant predicts mideclipse dates of HJD 2,440,664 for one cycle earlier and HJD 2,452,042 for one cycle later. The uncertainty of these predictions is about 240 days.

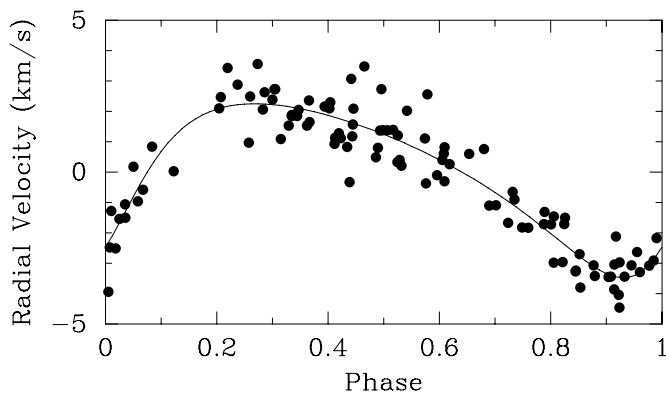


**Figure 3.** The computed velocity curve of the 2.1 yr velocity variation interpreted as an orbit, compared with the KPNO radial velocities. Each plotted velocity consists of the total observed velocity minus its calculated long-period velocity. Zero phase is a time of periastron.

#### 4. BASIC SYSTEM PARAMETERS

Paper I presented a broad introduction to CH Cyg, but much material has been published subsequent to that time. To understand the nature of the CH Cyg system, we first undertake an extensive review of the literature to determine basic parameters: variability, distance, luminosity, radius, rotation, mass, mass loss, and orbital inclination. This results in a revised picture of the system.

##### 4.1. Variability

The photometric variability of CH Cyg was reviewed by Muciek & Mikołajewski (1989) and Mikołajewski et al. (1990a). The mass-accreting component in the CH Cyg system contributes to the flux especially at blue wavelengths. During periods of strong activity, the M-giant variability can be cloaked even in the optical with light generated by the accretion process. However, during quiescent periods, the M giant can be detected into the blue.

CH Cyg had an extended period of quiescence from 1885 to 1963. During this interval, CH Cyg was known only as a late-type semiregular variable star. A review of historic material on the variability of CH Cyg by Muciek & Mikołajewski (1989), obtained during the period of quiescence, finds that the dominant period in the M giant is  $\sim 100$  days. During periods of symbiotic activity the 100 day period can be hard to detect (Mikołajewski et al. 1992; Munari et al. 1996). The visual amplitude of the 100 day period is small,  $\sim 0.1$  magnitude (Muciek & Mikołajewski 1989). The exact period depends on the dates sampled. Mikołajewski et al. (1990a) gave the dominant period as  $94$  and  $99 \pm 2$  days, while Mikołajewski et al. (1992) found  $102 \pm 3$  days. Mikołajewski et al. (1992) concluded that the  $\sim 100$  day period is systematically increasing at a rate of  $\sim 5$  days per century and suggested, following the work of Wood & Zarro (1981), that the CH Cyg M giant is currently undergoing a helium-shell flash. Mikołajewski et al. (1990a) and Mikołajewski et al. (1992) both noted that the  $\sim 100$  day period implies that the CH Cyg giant is a first overtone pulsator.

In addition to the 100 day period, a period of  $\sim 770$  days is also frequently reported. Mikołajewski et al. (1992) provided a detailed analysis of the 770 day photometric period in CH Cyg. The photometric properties of the 770 day variation show increasing amplitude toward shorter wavelengths, but not in a way consistent with dust extinction. In addition, the energy

distribution in the IR suggests changing spectral-type (and temperature) during the light cycle, but there are no spectral-type changes in the blue. While Munari et al. (1996) failed to detect this period, Skopal et al. (2007) noted the presence of a  $\sim 750$  day period with an amplitude of nearly 1 mag in  $V$  photometry. The  $\sim 750$  day period is apparent in data illustrated in Skopal et al. (2007). The symbiotic was quiescent at the time of these observations. There is also a suggestion of the  $\sim 100$  day period in these data, but the spacing of the data is too coarse for the period to be adequately sampled.

The simultaneous presence of both periods in CH Cyg was reported by Payne-Gaposhkin (1954). She listed CH Cyg as one of the families of pulsators, with an LSP and estimated a typical long-to-short period ratio of  $\sim 9$  for these objects. A longer list of LSP semiregular variables appears in Houk (1963). Wood et al. (2004) asserted that the LSP stars listed in Payne-Gaposhkin (1954) and Houk (1963) are those with the largest amplitude secondary periods. The Houk (1963) catalog contains only  $\sim 1.5\%$  of the then known long-period variables. More recently, the fraction of local long-period variables with LSPs is reported by Percy et al. (2004) and Wood et al. (2004) as  $\sim 25\%$ – $30\%$ .

In Paper I, we noted the close agreement between the 770 day photometric period and the 750 day spectroscopic period and assumed that both originate from the same physical mechanism. We make the same assumption in this paper. Hinkle et al. (2002), Olivier & Wood (2003), and Wood et al. (2004) detected LSP variations spectroscopically in a number of semiregular variables. The semiregular 100 day pulsation was not detected spectroscopically. Scaling from typical ratios of velocity to photometric amplitude for SRb variables (Lebzelter et al. 2000), the CH Cyg 0.1 magnitude visual amplitude implies a  $\sim 0.5$  km s $^{-1}$  velocity amplitude. This is near the detection limit for our observations (Section 3).

#### 4.1.1. Eclipses

When the accretion disk in the CH Cyg system is active, light from the disk dominates the blue and violet portions of the spectrum. At such times, the optical light curve is highly complex. Eyres et al. (2002) present a summary of recent optical photometry. Because CH Cyg has a complex light curve, evidence for eclipses depends critically on collaborating evidence rather than just sudden decreases in the  $U$ -band light. The first claim of an eclipse of the hot component by the red giant, occurring from 1985 May to October, was reported by Mikołajewski et al. (1987). This was largely based on timing, matching a  $U$ -band event to one more than 15 years earlier. However, these decreases in light show a considerable structure because of activity in the system. The dates of mideclipse are JD 2440585 and JD 2446270, with the eclipse FWHM  $\sim 200$  days. The ingress is brief, perhaps 10 days. Mikołajewski et al. (1990a) reported an ephemeris of  $JD_{\min} = 2,446,275(\pm 75) + 5700(\pm 75)E$ .

Subsequent to the claim of Mikołajewski et al. (1987), considerable evidence has been published that supports the claim that the 1985  $U$ -band decrease is an eclipse. Skopal et al. (1996a) summarized a list of five changes in the CH Cyg system that were observed during the 1985 eclipse. These are (1) the disappearance of rapid optical flickering, (2) the dominance of the M-giant continuum in optical spectra at mideclipse, (3) the transition of double-peaked Balmer emission lines to weak broad single-peaked emission lines at mideclipse, (4) the

dominance of the red side of the double-peaked emission in  $H\alpha$  and  $H\beta$  before mideclipse and the dominance of the blue emission following mideclipse, and (5) the prominence of the nebular lines [Ne III] 3869 Å and [O III] 5007 Å. Items (1) and (2) show that the accretor was eclipsed. Items (3) and (4) identify the eclipsed object as a rotating disk. Item (5) shows that the blue-ultraviolet flux level was depressed during the eclipse so that nebular lines became visible.

Apparent confirming proof of eclipses in CH Cyg comes from the prediction and then observation of the eclipse of 1999 (Eyres et al. 2002; Sokoloski & Kenyon 2003b). Eyres et al. (2002) presented  $UBV$  photometry for the 1999 eclipse, revealing that the eclipse is not visible at  $V$ , but is clearly detectable in  $B$  and much more pronounced in  $U$ . This is the expected enhancement of an eclipse of a hot object by a cool star. In addition, they find that flickering is again absent during the 1999 eclipse, just as in 1985. The strengths of various accretion-related spectral lines decreased during the eclipse. From Figure 5 of Skopal et al. (2007) the mid-date of the eclipse in 1999 is estimated as JD 2,451,425.

A major complication to this recent eclipse identification is that the 1999 eclipse date, JD 2,451,425, is 550 days earlier than predicted by the ephemeris of Mikołajewski et al. (1990a) and 617 days earlier than our ephemeris. These differences correspond to an orbital phase shift of  $\sim 0.1$ . In eclipses of symbiotic stars, the observed eclipse is not that of the white dwarf, which is unobservable at visual wavelengths, but rather of a UV bright, hot spot. Three-dimensional simulations of the symbiotic-recurrent nova RS Oph by Walder et al. (2008) predict an accretion disk that has a diameter 0.1 times the major axis of the binary system. This accretion disk is surrounded by a much larger Archimedean spiral, so there is a large area over which the hot spot can occur. From observations of several symbiotics, Skopal (1998) concluded that during quiescent phases of the systems, the times of eclipses occur prior to the time of inferior conjunction of the giant. When the systems are active, eclipses coincide with conjunctions predicted by spectroscopic orbits. For CH Cyg, the Mikołajewski et al. (1990a) ephemeris from active periods agrees with the times of inferior conjunction given in Equation (1). The 1999 eclipse took place during the period of declining activity, preceding the current extended period of quiescence (Eyres et al. 2002; Skopal et al. 2007). We suggest that the accretion disk was undergoing changes at the time of the 1999 eclipse.

The details of the light-curve shape and hydrogen-line profiles in these eclipses add further support to the eclipse interpretation. In all cases, the  $U$  light is brighter before the eclipse than after. In cataclysmic systems, this is a well known eclipse hallmark. The pre-eclipse brightening results from the accreting side of the disk, facing the mass-donating star and rotating in the direction of orbital motion. For  $H\alpha$  and  $H\beta$  line profiles, observed through eclipse (Eyres et al. 2002; Fernie et al. 1986), the negative side of the profile is eclipsed first and reappears first. Thus, the accretion disk is rotating with the side moving away from the red giant on the leading side of the orbit.

The eclipses discussed above are associated with the 15.6 year orbit. Yet another complication in the discussion of CH Cyg eclipses is that Skopal (1995), Skopal et al. (1996a), and subsequent papers by Skopal claim that there are also eclipses in the 2.1 year orbit. Skopal (1995) reported the presence of  $U$ -band decreases spaced at  $\sim 2.1$  year intervals on the light curve. Supporting evidence is seen in the disappearance of flickering during at least some of these events. Counter to the 2.1

yr eclipse claim Mikołajewski et al. (1990b) and Sokolowski & Kenyon (2003b) found a general correlation of the strength of the flickering with the luminosity of the blue–violet continuum. Sokolowski & Kenyon (2003a) suggested that the events observed by Skopal et al. (1996a) are not eclipses but result from collapses of the inner accretion disk.

#### 4.1.2. Flickering and Jets

Flickering is an indicator of a compact mass-accreting object in the system. Mikołajewski et al. (1990b) found that the rapid optical variations (flickering) of CH Cyg have a period of  $\sim 500$  s. There is a range in the periods reported for optical flickering in CH Cyg, e.g., Hoard (1993) and Rodgers et al. (1997) suggested a period in the range  $\sim 2200$ – $3000$  s (for a detailed discussion see Sokolowski & Kenyon 2003b). With any of these timescales, the flickering must originate at a hot component in the CH Cyg system, since the dynamical timescale for the giant,  $t_{\text{dyn}} \sim (R^3/2GM)^{1/2}$ , is on the order of a month. Flickering is also seen in X-ray observations, confirming the white dwarf nature of the secondary (Ezuka et al. 1998).

CH Cyg is known to have both radio (Taylor et al. 1986) and optical (Solf 1987) jets, which are approximately in the plane of the sky. This provides a first limit on the inclination of the orbit, although the information from the eclipses is far more accurate. Crocker et al. (2002) found from a time series of observations that the jet is precessing with a period  $\sim 18 \pm 0.5$  yr. While the precession mechanism is uncertain, the period of the precession is similar to the 15.6 year orbit, suggesting that the white dwarf is in that orbit.

Sokolowski & Kenyon (2003a) discussed the relation between the inner disk and the development of jets. They argued that it is impossible to understand the jet and the optical activity of CH Cyg without an accretion disk around a white dwarf companion. Sokolowski & Kenyon (2003a) pointed out a strong correlation between optical flickering in CH Cyg and changes in flux. The decrease or disappearance of flickering corresponds to a decrease in the blue flux. They found that this is related to disruption of the inner disk and follows episodes of jet production.

### 4.2. Distance, Luminosity, and Radius

#### 4.2.1. Giant

Kenyon & Fernandez-Castro (1987) undertook a detailed photometric calibration of symbiotic spectral types. From the resulting type of M6.5 ( $\pm 0.3$ ) III for CH Cyg, Mürset et al. (1991) used a spectroscopic parallax to derive a distance of  $240^{+30}_{-20}$  pc. This is in excellent agreement with the  $268 \pm 66$  pc distance based on Hipparcos observations (Viotti et al. 1997), which has been used extensively in the literature since 1997. Recently, van Leeuwen (2007) reanalyzed the Hipparcos parallaxes resulting in a distance for CH Cyg that is nearly 10% closer,  $244^{+49}_{-35}$  pc, than the Viotti et al. (1997) distance. The uncertainties for the original and revised Hipparcos distances have large overlap.

Biller et al. (2006) provided a fit to optical and infrared photometry of CH Cyg, using a Kurucz model spectrum for an M6 III star and a dust model. They found a luminosity of  $6900 L_{\odot}$ . This is in good agreement with the value given by Skopal (1997) from an energy distribution encompassing the UV through the far-IR. He determined a bolometric luminosity of  $\sim 8000 \pm 4000 L_{\odot}$  for a distance of  $268 \pm 66$  pc. This luminosity corresponds to a radius of  $\sim 310 R_{\odot}$ .

Dyck et al. (1998) measured a 10.4 mas diameter for CH Cyg at  $2.2 \mu\text{m}$ . Assuming the 244 pc distance, the stellar radius is then  $273 R_{\odot}$ . Schild et al. (1999) found a radius of  $280 \pm 65 R_{\odot}$ , based on near-IR photometry. The Dyck et al. (1998) radius can also be calibrated to an effective temperature of  $3084 \pm 130$  K. This compares very well with the Richichi et al. (1999) calibration for spectral-type M 7 of  $3150 \pm 95$  K.

CH Cyg has a variable  $K$  mag ranging from  $\sim -0.9$  to  $-0.3$  (Munari et al. 1996). We adopt the mean as a typical magnitude,  $K = -0.6$  and  $J-K = 1.6$ . Taranova & Shenavrin (2007) reported  $K$ -band fading, with  $K$  as faint as  $+0.35$  and  $J-K = 2.06$ , but this appears to be related to dust formation episodes. With the 244 pc distance,  $K = -0.6$  corresponds to an absolute  $K$  magnitude of  $-7.5 \pm 0.4$ . The  $K$ -band bolometric correction can be computed from the  $J-K$  color, following Bessel & Wood (1984), to yield a bolometric magnitude of  $-4.3$  and a luminosity of  $4200^{+2000}_{-1500} L_{\odot}$ . Assuming a temperature of 3100 K, the effective temperature–radius–luminosity relation gives a radius of  $\sim 224 R_{\odot}$ .

The values of the M giant’s basic parameters, derived from the various analyses discussed above, are in reasonable agreement. For the following discussion, we adopt values of  $L \sim 5000 L_{\odot}$ ,  $T \sim 3100$  K, and  $R \sim 280 R_{\odot}$ . The corresponding bolometric magnitude is  $-4.5$ . We note that typical radii for other giant stars in symbiotic binaries of earlier spectral types are 100–200  $R_{\odot}$  (Fekel et al. 2003).

#### 4.2.2. White Dwarf

While the white dwarf in the CH Cyg system has not been observed directly, some properties can be inferred from the accretion process. As summarized by Karovska et al. (2007), X-rays from CH Cyg have been detected by a number of groups. The X-rays originate from the accretion disk–white dwarf boundary layer as well as from a shock, where the jet interacts with circumbinary material. Ezuka et al. (1998) used X-ray spectroscopy to determine the temperature and bolometric luminosity of the white dwarf. The luminosity derived,  $\sim 10^{33}$  ergs  $\text{s}^{-1}$  ( $\sim 0.25 L_{\odot}$ ), can be combined with a mass–radius relation to set a lower limit on the mass of the white dwarf of  $0.44 M_{\odot}$ .

#### 4.3. Rotation and Line Widths

Schmutz et al. (1994), Mürset et al. (2000), and Zamanov et al. (2007) argued that in most S-type symbiotics, the giant star is synchronously rotating. In the case of synchronous rotation, the projected rotational velocity of the late-type giant can be used to estimate the stellar radius (e.g., Fekel et al. 2008). The  $v \sin i$  value for the M giant can be estimated from the FWHM of unblended absorption lines in the near-infrared spectra. Using atomic lines near  $2.223 \mu\text{m}$ , we apply the analysis technique of Fekel (1997) to CH Cyg. For CH Cyg, an empirical calibration with intrinsic line broadening of  $3 \text{ km s}^{-1}$  yields  $v \sin i$  of  $8 \pm 1 \text{ km s}^{-1}$ .

Both the 15.6 year and 2.1 year orbits of CH Cyg are eccentric. In an eccentric orbit, the rotational angular velocity of the M giant synchronizes with the orbital angular velocity at periastron. This was called “pseudo-synchronization” by Hut (1981). Using equation (42) of Hut (1981), we calculate a long pseudo-synchronous period of 5219 days and a short pseudo-synchronous period of 453 days.

Assuming  $\sin i = 1$ , the stellar equatorial rotational velocity is  $8 \text{ km s}^{-1}$ . Combining this value with the pseudo-synchronous

periods, (Fekel et al. 2003) suggested a stellar radius of  $825 R_{\odot}$  for the 15.6 year orbit or  $72 R_{\odot}$  for the 2.1 year orbit. The two computed radii are in poor agreement with the  $\sim 280 R_{\odot}$  value from the direct measurement of the stellar angular diameter. Thus in both the long- and short-period cases, the rotation of CH Cyg is not pseudo-synchronous. Other symbiotic systems with orbital periods near that of the short period are synchronized (Fekel et al. 2003; Zamanov et al. 2007).

In Paper I, we found that for CH Cyg lines of modest strength, the FWHM varies by  $\sim 30\%$  over the 2.1 year period. The pseudo-synchronous period differs by nearly a factor of 2 from the spectroscopic period. However, the line-width modulation is clearly occurring with the 2.1 year period. The rotational broadening would be more than twice that observed for a period of 2.1 yr and a diameter equal to that of CH Cyg. We conclude that the variation in the line widths is not due to a rotational modulation associated with star spots or plages.

#### 4.4. Masses

The values for the stellar parameters of CH Cyg can be used with stellar evolution theory to place additional constraints on mass. Schmidt et al. (2006) determined a solar iron abundance for CH Cyg. From Table (2) of Vassiliadis & Wood (1993), the solar abundance and a bolometric magnitude of  $-4.5$  for CH Cyg yield an initial mass for the M giant between  $\sim 1.5$  and  $3.5 M_{\odot}$ . Other arguments also suggest a mass near  $2 M_{\odot}$ . If CH Cyg is currently undergoing a helium-shell flash (Section 4.1), the luminosity is currently near a peak, which requires a mass near the bottom of the mass range. Based on the absolute magnitude and effective temperature, Schmidt et al. (2006) found  $\log g \sim 0$  for the surface gravity of CH Cyg. This also is in agreement with a mass of  $2 M_{\odot}$  for a radius of  $280 R_{\odot}$ .

If we assume that the white dwarf is not the result of a pathological evolutionary process, then the relation of Kalirai et al. (2008) can be used to map the white dwarf initial to final mass. The initial mass of the white dwarf, which evolved from the more massive star in the binary, had to be larger than the initial mass of the current M giant, requiring the mass of the white dwarf to be  $>0.56 M_{\odot}$ .

#### 4.5. Mass Loss

Gas- and dust-mass-loss rates for a number of symbiotics, based on *IRAS* photometry, are given by Kenyon et al. (1988). Revising the distance to 244 pc, the dust-mass-loss rate of CH Cyg is  $4 \times 10^{-7} M_{\odot} \text{ yr}^{-1}$ , and the gas-mass-loss rate is  $1 \times 10^{-8} M_{\odot} \text{ yr}^{-1}$ . A mass-loss rate for dust, based on near-IR photometry, was computed by Taranova & Shenavrin (2004) and Taranova & Shenavrin (2007). They obtained  $\sim 3 \times 10^{-7} M_{\odot} \text{ yr}^{-1}$  in good agreement with Kenyon et al. (1988). A dust formation episode in late 2006 resulted in multiple magnitude dimming in the *J*, *H*, and *K* bands plus dimming of a few tenths of a magnitude at *L* and *M*. Assuming a spherical symmetry for the dust shell, Taranova & Shenavrin (2007) translated the brightness change into a mass-loss rate of  $2 \times 10^{-5} M_{\odot} \text{ yr}^{-1}$ .

Kenyon et al. (1988) derived a dust temperature of 400 K, considerably less than the value of 750–800 K, given by Taranova & Shenavrin (2004). The radius of the dust scales inversely to the dust temperature (Kenyon et al. 1988). From Kenyon et al. (1988), Equation (5),  $R_d \sim 108$  AU for 400 K dust and 19 AU for 800 K dust. The semimajor axis of the 15.6 year orbit is on the order of 8 AU, so the dust at either temperature lies well outside the stellar orbits.

Mid-infrared imaging shows a Gaussian dust shell of  $\sim 45$  AU FWHM (Biller et al. 2006). This confirms the circumbinary nature of the dust and suggests that the dust temperature is between the Kenyon et al. (1988) and Taranova & Shenavrin (2004) values and in the same temperature range as found in D-type systems (Kotnik-Karuzza et al. 2007). Because the dust is circumbinary, counter to the assumption of Taranova & Shenavrin (2007), extinction events are no doubt due to localized condensations (clouds) rather than large-scale mass ejection events.

#### 4.6. Inclination

Fekel et al. (2008) noted that the minimum inclination for symbiotic eclipses is given by

$$\cos(i) < (R_{\text{rg}} + R_{\text{wd}})/a, \quad (2)$$

where  $a$  is the semimajor axis of the binary,  $i$  is the orbital inclination, and  $R$  is the radius of the red-giant and white dwarf components. From Section 4.2.1,  $R = 280 R_{\odot}$ . From the orbital elements, the red-giant semimajor axis can be determined, but it is the total semimajor axis that is required for Equation (2), so a total mass must be assumed. For a first estimate, we adopt the total mass from stellar evolution (Section 4.4) of  $2.5 M_{\odot}$ . Then from Kepler's third law and the 15.6 year period, the semimajor axis is 8.5 AU, resulting in a minimum inclination of  $81^{\circ}$ . With this estimate for the inclination,  $\sin i$ , which is critical to converting the observed mass function into component masses, is equal to 1.0 to better than 2%.

The length of the eclipse gives more precise information about the inclination. The eclipse duration is  $\sim 200$  days (Mikołajewski et al. 1987). Ingress/egress is short compared to the length of the eclipse, as expected, if the size of the eclipsed UV bright spot is much smaller than the diameter of the red giant. The 15.6 year orbit has a small eccentricity of 0.122, and, so for simplicity, we assume the orbit is circular. The eclipse duration is then 3.5% of the orbital period. For a semimajor axis of 8.5 AU, the white dwarf moves  $404 R_{\odot}$  during an eclipse. This value sets a lower limit on the diameter of the red giant.

We can compute the inclination by comparing the distance moved during the eclipse with the  $280 R_{\odot}$  radius of the giant. From geometry, the white dwarf traverses a path  $194 R_{\odot}$  off the center of the M giant, giving an inclination of  $84^{\circ}$ . This is in agreement with an estimate by Skopal (1995) of  $i > 83^{\circ}$ , based on the shape of the 1985 eclipse and the assumption of  $R_{\text{rg}} = 200 R_{\odot}$ .

#### 4.7. Summary of Basic Parameters

From the above sections, we can distill a profile of the components of CH Cyg. The M-giant velocities show the existence of both a short-period (2.1 yr) and long-period (15.6 yr) "orbit." However, only two stars have been identified directly or indirectly in the CH Cyg system, an M giant and a white dwarf. The M giant has  $L \sim 5000 L_{\odot}$  ( $M_{\text{bol}} = -4.5$ ),  $T \sim 3100$  K,  $R \sim 280 R_{\odot}$ , and  $M \sim 2 M_{\odot}$ . The white dwarf has  $M_{\text{wd}} > 0.6 M_{\odot}$ . The M giant has solar abundances, is on the thermal pulsing asymptotic giant branch (AGB), and is a radial overtone pulsator with a period of  $\sim 100$  days. The CH Cyg long-period system has an orbital period of 15.6 yr, eclipses, and has an inclination of  $84^{\circ}$ . These data are summarized in Table 3.

**Table 3**  
Derived CH Cyg Component Parameters

Parameter	Value	Reference
	Red Giant:	
$M_{\text{bol}}$	-4.5	Section 4.2.1
$L$	$5000 L_{\odot}$	Section 4.2.1
$T$	$3100 K$	Section 4.2.1
$R$	$280 R_{\odot}$	Section 4.2.1
$M$	$2 M_{\odot}$	Section 4.4
	White Dwarf:	
$L$	$0.25 L_{\odot}$	Section 4.2.2
$M$	$>0.56 M_{\odot}$	Section 4.4
	Long Period Orbit:	
$P$	15.6 yr	Section 3
$a$	8.5 AU	Section 4.6
$i$	$84^{\circ}$	Section 4.6
	Circumstellar Shell:	
$R_{\text{inner}}$	22 AU	Section 4.5

## 5. MODELS OF THE CH Cyg SYSTEM

Several models have been proposed to explain the observed properties of the CH Cyg system. In the following sections, we briefly review and comment on these models.

### 5.1. Mikołajewski et al. (1987)

From the rather poor radial velocities available at that time, Mikołajewski et al. (1987) concluded that CH Cyg is a binary with a period  $\sim 5700$  days and a large orbital eccentricity of 0.55. While we have confirmed the period, our radial velocities result in a greatly reduced eccentricity. Mikołajewski et al. (1987) estimated that the system consists of an M6 giant with a mass of  $\sim 3 M_{\odot}$  and a white dwarf companion with a mass  $\sim 1 M_{\odot}$ . The white dwarf is surrounded by an accretion disk formed from the red-giant wind. Eclipses were identified in *U*-band light curves, and as a result, the inclination was set to  $90^{\circ}$ .

### 5.2. Hinkle et al. (1993)

Hinkle et al. (1993, Paper I) demonstrated that the CH Cyg system has two independent sets of velocity variations, a 2.1 year short period, and a  $\sim 15$  year long period. They noted that other well known symbiotic systems have orbits of about two years and that CH Cyg can exhibit large amounts of activity associated with mass transfer to the secondary. This was presumed to imply a small orbital separation. In addition, at this time (early 1990s) the evidence for eclipses was weak. To devise a model similar to other active symbiotic systems, it was proposed that the components of the symbiotic system reside in the short-period orbit.

Paper I then used the mass function (Russell et al. 1955),

$$f(m) = (m_{\text{wd}}^3 \sin^3 i) / (m_{\text{rg}} + m_{\text{wd}})^2, \quad (3)$$

where  $m_{\text{wd}}$  is the mass of the white dwarf,  $m_{\text{rg}}$  is the mass of the red giant, and  $i$  is the orbital inclination, to derive limits on the masses and inclination. Constraining the inclination by the requirement that the observed jet is nearly in the plane of the sky required a very low-mass white dwarf. The third star in the long-period orbit was assumed to be an unseen late-type dwarf. The model presented in Paper I was based on a moderate inclination. As discussed in the present paper, this model is no longer tenable due to improved knowledge of the component masses and orbital inclination.

### 5.3. Skopal et al. (1996)

Skopal et al. (1996a) claimed that both long- and short-period eclipses are present in optical photometry and spectroscopy. They then proposed a revised three-body model. Skopal et al. (1996b) felt that similarities between the 2.1 year period of CH Cyg and other symbiotic systems require that the symbiotic system be in the short-period orbit. To produce the observable eclipses, the G-K dwarf in Paper I was replaced with a giant in the long-period orbit. In recognition of the single-lined nature of the spectrum, Skopal (1997) argued that the spectrum of the giant in the long-period orbit is blended with the M7 III primary, and one of the two giants is a bright giant. Taranova & Shenavrin (2004) suggested that the giants be nearly identical.

This model has several problems. Mikkola & Tanikawa (1998) found a triple system with a giant in the outer orbit to be unstable. There is no evidence in the spectra for the other bright giant. If two giants are present in the system, stellar evolution requires that they have nearly identical masses. In this case, the inclination required by the mass function is relatively small, and eclipses from the inner orbit will not occur.

### 5.4. Mikkola & Tanikawa (1998)

Mikkola & Tanikawa (1998) proposed that there is an inner close binary of total mass  $\sim 4 M_{\odot}$  with a white dwarf of mass  $\sim 1 M_{\odot}$  in an outer orbit. The inner orbit is at a high inclination with respect to the white dwarf orbit. Activity on the white dwarf is driven by a Kozai resonance which causes large eccentricity variations in the inner binary. In the high-eccentricity state, gas would be expelled from the red giant, causing activity on the white dwarf. This model explains the long periods of inactivity in CH Cyg.

The masses of the Mikkola & Tanikawa (1998) model are not in agreement with the derived masses for the system, but the basic model is potentially viable. We will return to this point in discussing binary models for the short period variation.

### 5.5. Two-Star Models

Munari et al. (1996) registered several objections to the triple-star model for CH Cyg. These included orbital stability, proposed masses for the components, and modeling the photometric behavior. They suggested that the short-period variations are pulsational, and hence, the system must be a binary. However, Munari et al. (1996) failed to note that a 2.1 year pulsation exceeds the fundamental period. Thus, if the 2.1 year period results from pulsation, it can be neither a normal pulsation mode of the star nor a beat between pulsation modes.

Ezuka et al. (1998) derived a minimum mass of  $0.4 M_{\odot}$  for the white dwarf, which exceeds the limit imposed in Paper I. They concluded that the value of the mass function determined in Paper I is implausible. While their minimum white dwarf mass is indeed inconsistent with the result for the 2.1 year orbit, Ezuka et al. (1998) failed to note that Paper I presented both short- and long-period mass functions, and the latter value is consistent with the  $0.4 M_{\odot}$  white dwarf mass limit.

Schmidt et al. (2006) briefly reviewed the controversy about whether the CH Cyg system is a triple or binary system. They also discussed whether the white dwarf is in the inner or outer binary. They noted the discovery that radial velocity variations of multiple-mode semiregular M-giants have periods longer than the fundamental radial mode (Hinkle et al. 2002). Indeed, CH Cyg has a strong similarity to these systems, which suggests that the 2.1 year period in CH Cyg could be a nonradial pulsation

mode. If so, the long-period velocity variation discussed in Paper I must correspond to the orbit containing the symbiotic components, and the CH Cyg system is a binary not a triple system. This is a viable model for the CH Cyg system, and we will examine this possibility more extensively below.

## 6. THE CH Cyg SYMBIOTIC SYSTEM

Adopting  $\sin^3 i = 1$  and using the masses of 2.0 and 0.6  $M_{\odot}$  that were estimated in Section 4.4, we compute from Equation (3) a value for the mass function of 0.032  $M_{\odot}$ . This value is similar to our 15.6 year mass function value of 0.051  $M_{\odot}$ , but quite different from our 2.1 year mass function value of 0.0015  $M_{\odot}$ . Increasing the white dwarf mass to 0.72  $M_{\odot}$ , which implies a progenitor mass of 3.3  $M_{\odot}$  (Kalirai et al. 2008), produces a match to the 15.6 year mass function value of 0.051  $M_{\odot}$ . This mass function value is then in agreement with multiple lines of evidence, reviewed above, that require the symbiotic components to be members of the long-period system. For the above masses, Kepler's third law produces a semimajor axis of 8.7 AU. Assuming that the 15.6 year and 2.1 year orbits are coplanar and that the red-giant mass is 2.0  $M_{\odot}$ , the 2.1 year mass function requires a mass of  $\sim 0.2 M_{\odot}$  for a postulated secondary star in that orbit, a point that we will return to in discussing the nature of the short-period variation.

The masses of the dwarf and giant are, of course, related but not uniquely constrained by the 15.6 year mass function. From the various limits set on the values for the masses, the red-giant mass is in the range  $1.5 \leq M_{\text{rg}} \leq 3.0$ . From the long-period mass function, the corresponding range for the white dwarf is  $0.61 \leq M_{\text{wd}} \leq 0.92$ . Significantly, all the values for masses of the white dwarf derived from the long-period mass function are in accord with evolutionary constraints. The mass range is sufficiently small to exclude possible models for CH Cyg, with either low- or high-mass white dwarfs (see for example Luna & Sokolowski 2007).

Iben & Tutukov (1996) commented in their extensive paper on the evolution of symbiotic stars that symbiotic systems are a “nonuniform family of wide binaries, with actively interacting components that differ in (1) the nature of their accreting components, (2) reasons for mass exchange, and (3) the physical mechanisms for their observed variability.” This captures the difficulty in understanding CH Cyg. Although the system is phenomenologically similar to many S-type symbiotics, in many respects it is a different type of symbiotic system. The orbital period of 15.6 yr is more than three times that of the next longest S-type symbiotic with a well defined orbit (Fekel et al. 2007). In addition, none of the previously studied S-type symbiotics have a pulsating asymptotic giant branch (AGB) star in the system. The D-type symbiotics R Aqr and o Cet are fundamental AGB pulsators (Miras), while CH Cyg is an overtone AGB pulsator. Consequently, CH Cyg has a lower mass-loss rate than the fundamental mode Miras. However, in the CH Cyg system, the lower mass flow to the secondary is compensated by the smaller semimajor axis. The much less studied symbiotic PU Vul is possibly a similar system (Nussbaumer & Vogel 1996).

The Mira symbiotics R Aqr and o Cet are similar to CH Cyg in some respects. For example, R Aqr has a jet, although its 43.6 year orbital period is nearly three times that of CH Cyg. The R Aqr system semimajor axis is 14–17 AU (Gromadzki & Mikołajewska 2008). o Cet has a period more than 10 times longer,  $\sim 500$  yr, with 70 AU component separation (Prieur et al. 2002). o Cet exhibits flickering on the secondary with a timescale similar to that seen on CH Cyg (Warner 1972).

Such flickering is not a common feature of symbiotic systems. CH Cyg, R Aqr, and o Cet have all been detected at X-ray wavelengths (Karovska et al. 2007). No doubt the comprehensive information about these three objects, including the X-ray flickering, is also a measure of the detail in which these nearby objects can be studied. X-ray flickering could well be present in other systems, but is masked by other X-ray emission from the systems or by the larger distances to other systems.

It is interesting to compare the near-IR colors of CH Cyg, both outside and during dust-formation events, with the colors of symbiotic (D-type) Miras. The spectral type of CH Cyg is similar to that of many Miras near maximum light. Whitelock (1987) provides infrared photometry for a selection of symbiotic Miras. When quiescent, CH Cyg occupies the domain of normal Miras in a  $(J-K)-(K-L)$  relation. During a dust-formation episode, the CH Cyg colors evolve along the line occupied by symbiotic Miras. Of the symbiotic systems studied by Whitelock (1987), CH Cyg is most similar to Hen 2-38.

Whitelock (1987) found it unlikely that symbiotic systems, which currently contain Miras, would have been recognized as symbiotic prior to the onset of the Mira high-mass-loss phase. She also noted, as did Iben & Tutukov (1996), that there is not an evolutionary relation between symbiotics. Symbiotics are binary systems of different separations, passing through an evolutionary phase that results in mass transfer.

A question frequently raised about CH Cyg is the cause of the changes in the activity state of the symbiotic system. As discussed by Mikołajewski et al. (1990a), CH Cyg was quiescent from the first observations in 1885 until 1963. The interval since 1963 has been dominated by periods of activity mixed with quiescent periods. With a 15.6 year-binary orbit and normal M-giant mass loss, Mikołajewska et al. (1988) found that the Bondi–Hoyle accretion onto a  $\sim 1 M_{\odot}$  white dwarf from the giant wind was lower by about an order of magnitude than the accretion required to drive the hot-component luminosity.

A solution is that widely separated, high-mass-loss rate symbiotic systems are undergoing *wind Roche lobe overflow* (see for instance Podsiadlowski & Mohamed 2007). The stellar wind in these systems is directed by the Roche lobe, and the efficiency of mass transfer to the secondary is much higher than might otherwise be expected. Models suggest mass-transfer efficiencies approaching 100% instead of a few percent as previously believed. This addresses the active states but not the periods of inactivity. The latter have been attributed by Sokolowski & Kenyon (2003b) to the collapse of the inner accretion disk. We will discuss the activity of CH Cyg below in relation to the nature of the 2.1 year variation.

## 7. THE 2.1 yr PERIOD

In Paper I, we assumed that both the 2.1 year photometric and spectroscopic changes were due to orbital motion. With the recognition that the symbiotic system resides in the 15.6 year orbit, we seek an understanding of the 2.1 year periodic variation.

Semiregular variables obey a period–luminosity (P–L) relation (Wood & Sebo 1996). From MACHO data, a number of overtone series were identified in the LMC by Wood et al. (1999). Since the publication of this seminal work, the relations have been refined with data from other surveys, most recently those of OGLE (Soszyński et al. 2007). Linear pulsation periods calculated by Wood (2007) can be compared with the LMC data to identify the modes of pulsation. Period–luminosity sequences are present for fundamental through fourth overtone pulsation.

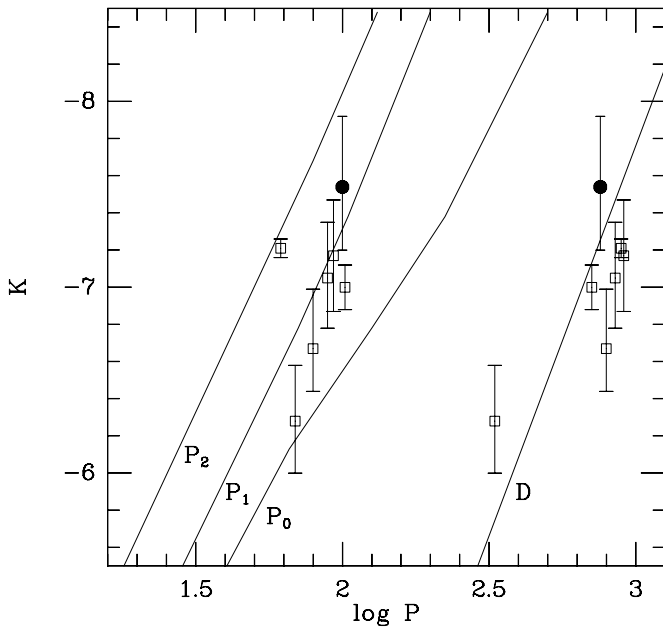


**Figure 4.** Period–absolute  $K$  magnitude plot of field LSP stars. Each LSP star has two periods, a normal pulsation mode and the LSP. Filled circle is CH Cyg. Open squares are six LSP stars from Hinkle et al. (2002) and Wood et al. (2004) that have Hipparcos parallaxes. The van Leeuwen (2007) revised *Hipparcos* parallax values are used. The lines  $P_0$ ,  $P_1$ , and  $P_2$  show respectively linear fundamental, first overtone, and second overtone pulsation periods from Wood et al. (1999) for oxygen-rich opacities. The line D is the middle range of the Wood’s D relation (see Wood et al. 1999). For field stars the uncertainty in the distance, indicated by the magnitude error bars, combined with the intrinsic range in magnitude blurs the observed pulsation relations, although most of these stars are clearly first overtone pulsators.

CH Cyg is well established as a semiregular variable with a period of  $\sim 100$  days. Its absolute  $K$  magnitude is  $-7.5 \pm 0.4$  (Section 4.2.1). To compare CH Cyg with the LMC relations found by Wood et al. (1999) and others, we take a distance modulus of 18.58 from Szcwzyk et al. (2008) for the LMC. The pulsation mode(s) of CH Cyg then can be identified from the appropriate period–luminosity relation. The CH Cyg 100 day period and magnitude are within 0.2 mag of the relation for first overtone pulsation (Figure 4). This is well within the  $\sim 0.5$  magnitude natural width of the relation (Soszyński et al. 2007).

In Section 4.1, the 2.1 year period was identified as a “long-secondary period” (LSP). LSP variables are so-named, because they all also have shorter period pulsation. LSP variables were found by Wood et al. (1999) to obey a P–L relation (his sequence “D”). The CH Cyg 2.1 year period is  $\sim 0.3$  magnitude off the center of the D sequence (Figure 4), but again well within the natural width of the relation. Wood et al. (1999) pointed out that the range in the ratio of the long-to-short period is a function of the long period and at periods near 1000 days ranges from 5 to 15. The long-to-short-period ratio for CH Cyg is  $\sim 8$ . Derekas et al. (2006) found that no normal stars fall between the fundamental and LSP sequences. Figure 4 illustrates that the 2.1 year CH Cyg period is clearly *not* fundamental pulsation.

While approximately 25%–30% of all pulsating AGB stars show LSP behavior (Wood et al. 1999; Percy et al. 2004), there is considerable disagreement about the physical cause. Possible origins of the LSPs have been investigated by Hinkle et al. (2002), Olivier & Wood (2003), Wood et al. (2004), Derekas et al. (2006), and Soszyński (2007), among others. Six causes have been proposed: (1) radial pulsation, (2) nonradial pulsation, (3) a low-mass companion, (4) rotating-spheroidal shape for the

star as the result of common-envelope evolution, (5) circumstellar dust clouds, and (6) star spots. Of this list, two causes of the LSPs remain viable after detailed investigations by the above authors: orbital motion from a close, low-mass companion, and nonradial pulsation. Wood et al. (2004) concluded that the most likely explanation for the LSPs is a low degree  $g$  mode in the outer radiative layers of the AGB star. However, Soszyński et al. (2007) and others noted that the sequence D variables form an extension of the ellipsoidal variable sequence. This suggests that at least some LSPs result from extremely low-mass contact binaries.

CH Cyg appears on the Payne-Gaposhkin (1954) and Houk (1963) lists of LSP variables. While these authors knew that the long-to-short-period ratio was in the range of 5–15, the discovery that AGB variables have a period–luminosity relation did not occur for another 25 years (Feast et al. 1989), and the identification of the LSP period–luminosity relation followed 10 yr later (Wood et al. 1999). Thus, it is not surprising that the 2.1 year period in CH Cyg has not been extensively investigated as a possible LSP. However, it turns out that some of the same arguments, which have been investigated as possible causes of LSP variability, have been investigated for CH Cyg. Based on the specifics of the 770 day photometric variability, Mikołajewski et al. (1992) concluded that the 770 day period is not caused by variable extinction, as previously proposed by Mikołajewski et al. (1990a). Mikołajewski et al. (1992) also dismissed rotation as a cause, since the rotational velocity required is  $\gtrsim 13 \text{ km s}^{-1}$  and would produce noticeable line broadening. In Section 4.3, the CH Cyg line width was shown to be slightly more than half this value. Mikołajewski et al. (1992) hypothesized that the 2.1 year period might be the result of spots related to cyclic changes in convective cells. This origin for LSP behavior was ruled out by Wood et al. (2004).

### 7.1. Binary Hypothesis

Soszyński et al. (2004) and others show that the sequence of ellipsoidal variables (sequence E) overlaps Wood’s sequence D. The period–luminosity relation requires that binary systems causing D sequence photometric variations be contact binaries (Derekas et al. 2006). Based on the shape of the light and velocity curves, it is apparent that the short-period system in CH Cyg is not a standard contact binary. Velocity curves for various contact binary systems can be found in Lu & Rucinski (1999) and Wood (2007). Contact binary radial velocity curves have a characteristically sinusoidal shape, because their orbits are circular. Adams et al. (2006) found the sequence E objects in their sample to be first ascent, giant branch objects with very small envelope masses, probably as the result of a common envelope mass ejection event. However, Soszyński (2007) noted that if the Roche lobes are not full, it is possible to transfer mass, driven by a stellar wind. In such a situation, the eccentricity can be increased. Thus, it is of interest to discuss the binary option for CH Cyg.

In our discussion of the symbiotic CH Cyg binary system, a number of arguments have been used to assign mass, effective temperature, and radius to the M giant (Section 4). In addition, the inclination of the 15.6 year orbit is known from eclipses to an uncertainty of less than a degree. We initially assume the simple case of coplanar 15.6 year and 2.1 year orbits. It is then possible to solve for the mass of a possible 2.1 year companion. Assuming a  $2 M_{\odot}$  primary, a putative 2.1 year companion would have mass  $0.2 M_{\odot}$ . Using the mass-spectral-type calibration of Baraffe & Chabrier (1996), the hypothesized low-mass companion is then

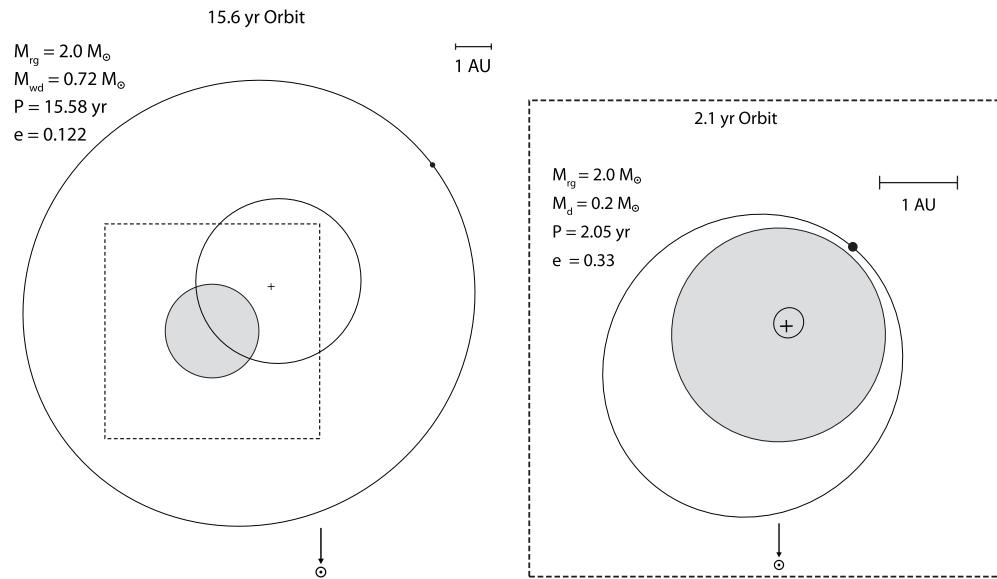


**Figure 5.** Polar view, to scale, of the computed orbits of the CH Cyg system. On the left, the inner and outer ellipses are the 15.6 year orbits with a red giant of mass  $2 M_{\odot}$  and a white dwarf of mass  $0.72 M_{\odot}$  (see text). The shaded circle and the dot represent the giant and white dwarf, respectively, at periastron. The shaded circle is the scaled size ( $R = 280 R_{\odot}$ ) of the red giant which is assumed spherical. The plus is the center of mass of the orbit. The dashed line box is shown enlarged on the right. The inner and outer ellipses are the 2.1 year orbits of the red giant and the low mass companion shown at periastron. The plus sign is the center of mass of the 2.1 year orbit. The 2.1 year and 15.6 year orbits are shown coplanar (see text). The companion object in the 2.1 year orbit cannot be a white dwarf. However, we argue (see text) that the 2.1 year orbit is not physical.

an M3 dwarf with an effective temperature  $\sim 3200$  K. This is so similar to the much more luminous M giant that such a dwarf would be undetectable spectroscopically. The Roche lobe radii of a  $2 M_{\odot}$  and  $0.2 M_{\odot}$  binary are  $260 R_{\odot}$  and  $96 R_{\odot}$ , respectively, in a circular orbit. However, the eccentricity  $e$  of the 2.1 year orbit is 0.33. Thus, the Roche lobe will be constantly changing from  $(1 + e)a$  for apastron to  $(1 - e)a$  for periastron. The radius of the giant is  $\sim 280 R_{\odot}$ , so such a system is Roche lobe filling, and so, at each periastron passage extreme mass loss would be expected.

In Paper I, instead of a main sequence red dwarf, a *white dwarf* companion of approximately  $0.2 M_{\odot}$  was hypothesized. We now argue that a  $0.2 M_{\odot}$  *white dwarf* companion cannot exist. The presence of a  $2 M_{\odot}$  star in the CH Cyg system requires that any progenitor of a white dwarf was initially more massive than  $2 M_{\odot}$ . Such stars produce white dwarfs that are more massive than  $0.6 M_{\odot}$  (Kalirai et al. 2008). However, we note that  $0.2 M_{\odot}$  white dwarfs do exist; Liebert et al. (2004) reported the discovery of such an object. Low-mass white dwarfs are believed to result from mass transfer and common envelope evolution with a degenerate companion. There seems no need to invoke this evolutionary path in the CH Cyg system. Even if such a white dwarf companion could exist, a contact system with an AGB star would be exceedingly active. In addition, the X-ray observations of CH Cyg result in mass limits which require a more massive white dwarf (Section 4.2.2).

Soszyński et al. (2007) found that the binary star explanation of the LSP requires the radius-to-semimajor-axis ratio to be  $\sim 0.4$ . Kepler's third law then requires a mass of  $6 M_{\odot}$  for the dwarf. However, masses larger than  $2 M_{\odot}$  are excluded if the stars in the system have equal ages. If the masses of the dwarf and the giant are equal the mass function requires an inclination of  $\sim 8^{\circ}$ . This, in turn, excludes the inclined orbit Kozai resonance model of Mikkola & Tanikawa (1998). On the other hand, a coplanar result is also evidence that the triple model is unphysical because triple systems are seldom, if ever, coplanar (Mutterspaugh et al. 2008).

The 2.1 year velocity variation (Figure 3) is not sinusoidal. This provides one of the most powerful arguments against the 2.1 year binary hypothesis. In fact, the eccentricity of 0.33 is moderately large. Polar views of the 15.6 year and 2.1 year orbits are shown in Figure 5. Soker (2000) provides formulae for computing the timescale for tidal synchronization. Because the low-mass companion does not have sufficient mass to spin up the envelope of the M giant, the synchronization timescale is the merger timescale,  $\sim 1000$  years (Wood et al. 2004). The timescale for orbital circularization is longer than the timescale for synchronized rotation. Merger in the synchronization timescale makes this argument mainly academic. However, the circularization timescale is also short,  $\sim 5000$  years, so all contact binary orbits of this type would be expected to be circular. As noted by Wood et al. (2004), there are many known LSP systems, so eccentric orbits, even if possible for one object, could not possibly be the case for the entire class.

Soszyński (2007) suggested that mass lost by the red giant in a binary system with a low-mass star follows a spiral pattern, producing the LSP variations. Such spiral mass loss could then affect the symbiotic binary system. However, as discussed in Section 4.5, infrared observations of CH Cyg require a dust temperature which places the dust well outside the the 15.6 year long-period orbit. Furthermore, Mikołajewski et al. (1992) found that the 770 day variation in CH Cyg, while color dependent, was inconsistent with reddening.

These arguments provide convincing evidence that the 2.1 year period variation of CH Cyg does *not* result from binary motion. For the entire LSP group, Derekas et al. (2006) used arguments based on a multivariate test of the amplitude–luminosity relation to conclude that the LSP phenomenon is, in general, not a result of contact binaries.

## 7.2. Pulsation

While it has been shown theoretically that radial pulsation cannot be a cause of the LSPs, this is still frequently listed

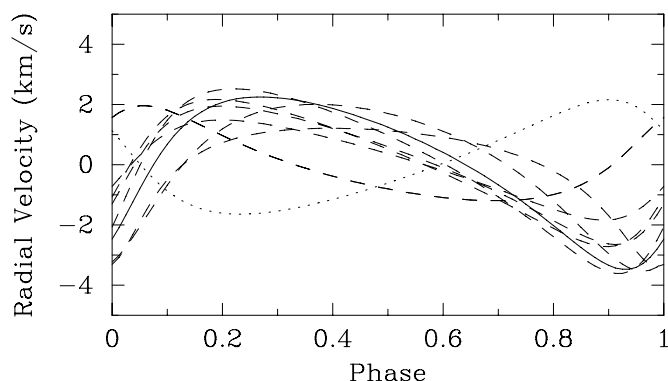


**Figure 6.** A phase plot of the calculated radial velocity “orbits” of long secondary periods for eight stars plus the 2.1 year period of CH Cyg. Six stars, RS CrB, AF Cyg, X Her, g Her, V574 Oph and BI Peg are from Hinkle et al. (2002), and two, Z Eri and S Lep, are from Wood et al. (2004). The center of mass velocity of each “orbit” has been subtracted from the observations to produce velocity curves with the same zero point for ease of comparison. The “orbit” of CH Cyg is a solid line, the other stars are dashed lines except for AF Cyg, which is a dotted line to emphasize that its “orbit” is in antiphase with the others.

among the possible causes. In the case of CH Cyg, several authors have suggested that the 770 day period is the result of the radial pulsation of the M giant (see Munari et al. 1996). We emphasize that a period of 770 days cannot possibly be a radial pulsation. The frequencies of radial pulsations in AGB stars can be calculated as a function of bolometric magnitude (Hughes & Wood 1990; Wood 2007). The fundamental period as a function of absolute  $K$  magnitude is plotted on Figure 4. At the luminosity of CH Cyg,  $K = -7.5$  mag, the radial fundamental period is  $\sim 250$  days. If the origin of the LSP is pulsational, the pulsations must be nonradial in nature.

Spectroscopic studies of LSPs have been carried out by Hinkle et al. (2002), Olivier & Wood (2003), and Wood et al. (2004). There are two remarkable qualities of the LSP velocities. First, the radial velocity variations among LSP stars are nearly identical. The velocity phase curves for seven LSP stars from Hinkle et al. (2002) and Wood et al. (2004) are shown in Figure 6. The position of these objects on the period–luminosity relation is shown in Figure 4. Although the original orbit for one of these stars, AF Cyg, had  $e = 0.08 \pm 0.20$ , given the large uncertainty, we have recomputed the orbit with  $e = 0.3$  as shown in Figure 6 and found a very acceptable fit to the velocities, even though the computed velocity curve is in antiphase with those of the other stars. The 2.1 year velocity phase curve of CH Cyg matches those of the other LSP stars. The remarkable similarity of the “orbits” is inconsistent with both the expectation of random orbital orientation and the circularization constraints discussed above. The variables included in Figure 6 are large visual amplitude LSP systems, so the similarity of velocity amplitudes could be a selection effect.

Second, the LSP velocity variations totally dominate the shorter pulsation period in the LSP objects studied. For instance, in CH Cyg, the overtone pulsations are not detectable in the velocities (Section 3) and result in only a low-amplitude photometric variation (Section 4.1). Thus, LSP velocity changes are not easily differentiated from orbital motion for stars where the photometric variation is poorly known. This could be pervasive among suspected binary systems. A possible example is the velocity curve of the X-ray, suspected neutron star symbiotic binary HD 154791 (Galloway et al. 2002), which matches the parameters of the LSP “orbits” of the stars in Figure 6.

As noted by Wood et al. (2004), velocity curves with the shape shown in Figure 6 can be reproduced by rotating prolate spheroids. The symmetry of such a spheroid requires a rotation period twice the period of the velocity curve. This period is in agreement with  $8 \text{ km s}^{-1}$  measured line widths in CH Cyg. Kiss et al. (2000) proposed a rotating-pulsating-ellipsoid model for the unusual light curves of two semiregular variables. A rotating-prolate spheroid could result from a recent binary merger, but it is difficult to understand how an entire class of variables following a period–luminosity law could be the result of recent mergers.

The observed properties of a rotating-prolate spheroid can be generated by low-order nonradial pulsation. In the case of nonradial pulsation, a period–luminosity relation would exist. Nonradial pulsation can be prograde, i.e., in the direction of stellar rotation, or retrograde. Unno et al. (1989) stated that waves traveling in retrograde, as opposed to prograde, result in identical velocity curves but with the sign reversed. This could explain the antiphase velocity curve of AF Cyg in Figure 6.

Hatzes (1996) provides models for some low- $l$  sectoral ( $l = -m$ ) modes. Unfortunately, the models are only for  $m = 2, 4,$  and  $6$ . For these modes, there are at least four sectors around the star and the velocity variations are nearly sinusoidal. The velocity amplitude decreases with increasing  $m$ , because for higher  $m$  there are a larger number of velocity zones, with cancelling sign (Hatzes 1996). The amplitude and asymmetry of CH Cyg suggest an  $l = 1$  mode. From the relations given by Hatzes (1996), the  $l = 1$  mode pulsation velocity amplitude is about half of the observed velocity amplitude. An interesting aspect of nonradial modes is that the vertical scale height is small.

Additional insight into the LSP problem comes from K to early M red giants. For these stars, Henry et al. (2000) reported the presence of short period, i.e. timescales of a few days to weeks, radial and nonradial pulsations. Henry et al. (2000) found nonradial pulsations restricted to the hot side of the coronal dividing line at about K2. For an early K giant, the radial periods are typically days. The K giants have secondary periods with lengths of hundreds of days. There is considerable uncertainty about the origin of the LSPs for these stars, as for the M-giant LSPs. As is the case for AGB LSPs, rotation with star spots, nonradial pulsations, and low-mass companions have been discussed as explanations. In the case of the K0 III star  $\pi$  Her, Hatzes & Cochran (1999) found the pressure scale height for the photosphere to be a factor of 10 smaller than the radial wavelength of the 613 day pulsations.

The hypothesis of nonradial modes in late-type giants has been impeded by the knowledge that gravity modes are evanescent in convective regions. This makes their postulated existence in both AGB and red giants difficult to understand. Thus, Hatzes & Cochran (1999) suggested  $r$ -mode oscillations (Wolff 1996), which arise in rotating, convective fluids, as an alternative. However, this alternative raises a different problem for AGB stars. In AGB stars, the rotational period results in a pulsation period which is too long. For  $r$  modes, the pulsation frequency is equal to the rotation frequency for  $l = 1$  and longer for higher modes (Wolff 1996). In the case of CH Cyg, the rotation period is more than twice the 2.1 year pulsation period. A solution proposed by Wood et al. (2004) relies on the point that LSP nonradial modes occur only in stars that also have radial pulsation. The proposal is that radial pulsation thickens the radiative layer above the convective layer, allowing the propagation of  $g$  modes.

Wood et al. (2004) discussed light and color variations in LSP stars. These can be compared with the variations in CH

Cyg (Section 4.1) and predictions from stellar pulsation. The reported changes in spectral-type are consistent with pulsation-related changes in temperature. The types of variation reported by Mikołajewski et al. (1992) are fully consistent with variations for other LSP stars and with variations expected from stellar pulsation (Wood et al. 2004).

A complication in understanding the CH Cyg system has been the report of short-period eclipses by Skopal et al. (1996a). Wood et al. (2004) concluded that for LSP stars, the strength of H $\alpha$  is a function of phase. They interpreted this as changing chromospheric activity. At some phases, the chromosphere is absent, while at other phases, it covers up to 70% of the stellar surface. This same phenomenon has been reported for the K-giant LSP stars. For  $\alpha$  Boo, the strength of He I 10830 Å is correlated with the LSP (Hatzes & Cochran 1993). We suggest that the UV changes in CH Cyg correlated with the short-period phase found by Skopal et al. (1996a) and Eyres et al. (2002) are pulsation-driven changes in the chromosphere. From the dates of the deep UV minima given in Skopal (1995), the 2.1 year orbital phase (from the eccentric orbit) is 0.14, which is conjunction in an orbital model or a time of null velocity movement in a pulsational model. The absence of flickering during at least some of these events could be unrelated changes of a structure in the white dwarf accretion disk (Sokoloski & Kenyon 2003a).

In Paper I, the change of the line shape with short-period phase was discussed. The spectral lines have the largest FWHM at  $\phi = 0.4$ – $0.6$ . However, the lines are more narrow and symmetric at phase 0.4, becoming more asymmetric at phase 0.8. For K giants, Hatzes (1996) noted the change in the bisector shape, with phase and mode being in nonlinear pulsations. The resolution and signal-to-noise ratio of the current CH Cyg spectra do not allow detailed comparison, but indicate that further study would be of interest.

A long-standing question for CH Cyg is why this star was an M-giant spectral-type standard for the first half of the 20th century and then became an active symbiotic star. At the heart of this question is the nature of the accretion onto the white dwarf secondary. A possibly naive expectation is that the LSP variation is a controlling factor in the M-giant mass loss. We speculate that in the case of a nonradial pulsation origin for LSP, the nonradial modes are stable but variations in the dominant mode can occur. If the dominant mode controls other stellar properties, for instance, the mass-loss rate or the directionality of the mass loss, the mass transfer in a symbiotic system would change. Observational tests employing samples of LSP variables should be possible.

## 8. CONCLUSIONS

The near-infrared radial velocities of CH Cyg conclusively show that the M giant in the system exhibits two different velocity variations: a 15.6 year “long” period and a 2.1 year “short” period. We have reviewed the literature on the basic parameters for the CH Cyg giant and have estimated its mass and radius. Evolutionary arguments require an M-giant mass near  $2 M_{\odot}$ . X-ray observations require a white dwarf companion more massive than  $0.44 M_{\odot}$ . Various lines of evidence but most compellingly observations of eclipses demand that the inclination of the 15.6 year orbit is nearly edge on. The long-period mass function is then matched by the assumption of a  $0.7 M_{\odot}$  white dwarf.

The CH Cyg symbiotic system is an unusual one. The separation between the giant and white dwarf is about four

times larger than that for typical S-type systems. CH Cyg is a first overtone pulsating AGB star, which will drive symbiotic mass transfer at a larger radius. While CH Cyg is classified as an S-type system, there are a number of similarities with D-type Mira systems. Changing activity in the CH Cyg symbiotic system is possibly related to variations in the short-period activity.

The observed 2.1 year velocity variation is indistinguishable from that seen in stars with LSPs. LSP objects occupy a track on the period–luminosity diagram, identified by Wood et al. (1999) as sequence D. The cause of the LSP variations, while discussed exhaustively, remains uncertain. LSP is the only theoretically unexplained type of stellar variability (Wood et al. 2004). In the case of CH Cyg, there seem to be only two viable options to produce the 2.1 year period. The star could be a rotating-prolate spheroid, perhaps as the result of a common envelope phase with a former low-mass companion. However, with this model, it is hard to understand why there are so many LSP stars. Much more likely, CH Cyg is undergoing low-order nonradial pulsations that mimic the observed properties of a rotating prolate shape. If these are  $g$  modes, the outer stellar structure of pulsating M giants does not follow standard models, because an outer radiative layer is required to propagate the  $g$  modes. While this structure change is not required for  $r$  modes, the periods of  $r$  modes are excessively long.

This research has been supported in part by NASA grant NCC5-511 and NSF grant HRD-9706268 to Tennessee State University. We have made use of the SIMBAD database, operated by CDS in Strasbourg, France, as well as NASA’s Astrophysics Data System Abstract Service. We thank D. Willmarth and D. Harmer for assisting at the KPNO coude feed telescope.

## REFERENCES

- Adams, E., Wood, P. R., & Cioni, M.-R. 2006, *Mem. S.A.It.*, **77**, 537  
 Baraffe, I., & Chabrier, G. 1996, *ApJ*, **461**, L51  
 Bessel, M. S., & Wood, P. R. 1984, *PASP*, **96**, 247  
 Biller, B. A., et al. 2006, *ApJ*, **647**, 464  
 Crocker, M. M., Davis, R. J., Spencer, R. E., Eyres, S. P. S., Bode, M. F., & Skopal, A. 2002, *MNRAS*, **335**, 1100  
 Daniels, W. 1966, Univ. of Maryland, Dept. of Physics & Astronomy Technical Report No. 579  
 Derekas, A., Kiss, L. L., Bedding, T. R., Kjeldsen, H., Lah, P., & Szabó, Gy. M. 2006, *ApJ*, **650**, L55  
 Deutsch, A. H., Lowen, L., Morris, S. C., & Wallerstein, G. 1974, *PASP*, **86**, 233  
 Dyck, H. M., van Belle, G. T., & Thompson, R. R. 1998, *AJ*, **116**, 981  
 Eyres, S. P. S., et al. 2002, *MNRAS*, **335**, 526  
 Ezuka, H., Ishida, M., & Makino, F. 1998, *ApJ*, **499**, 388  
 Feast, M. W., Glass, I. S., Whitelock, P. A., & Catchpole, R. M. 1989, *MNRAS*, **241**, 375  
 Fekel, F. C. 1997, *PASP*, **109**, 514  
 Fekel, F. C., Joyce, R. R., Hinkle, K. H., & Skrutskie, M. F. 2000, *AJ*, **119**, 1375  
 Fekel, F. C., Hinkle, K. H., & Joyce, R. R. 2003, in ASP Conf Ser. 303, *Symbiotic Stars Probing Stellar Evolution*, ed. R. L. M. Corradi, J. Mikołajewska, & T. J. Mahoney (San Francisco, CA: ASP), 113  
 Fekel, F. C., Hinkle, K. H., Joyce, R. R., Wood, P. R., & Howarth, I. D. 2008, *AJ*, **136**, 146  
 Fekel, F. C., Hinkle, K. H., Joyce, R. R., Wood, P. R., & Lebzelter, T. 2007, *AJ*, **133**, 17  
 Fernie, J.D., Lyons, R., Beattie, B., & Garrison, R. F. 1986, *IBVS*, 2935  
 Fitzpatrick, M. J. 1993, in ASP Conf. Ser. 52, *Astronomical Data Analysis Software and Systems II*, ed. R. J. Hanish, R. V. J. Brissenden, & J. Barnes (San Francisco, CA: ASP), 472  
 Galloway, D. K., Sokoloski, J. L., & Kenyon, S. J. 2002, *ApJ*, **580**, 1065  
 Gromadzki, M., & Mikołajewska, J. 2008, *A&A*, submitted (arXiv:0804.4139v1)

- Hall, D. N. B., Ridgway, S. T., Bell, E. A., & Yarborough, J. M. 1978, *Proc. SPIE*, **172**, 121
- Hatzes, A. P. 1996, *PASP*, **108**, 839
- Hatzes, A. P., & Cochran, W. D. 1993, *ApJ*, **413**, 339
- Hatzes, A. P., & Cochran, W. D. 1999, *MNRAS*, **304**, 109
- Henry, G. W., Fekel, F. C., Henry, W. M., & Hall, D. S. 2000, *ApJS*, **130**, 201
- Hinkle, K. H., Cuberly, R., Gaughan, N., Heynssens, J., Joyce, R., Ridgway, S., Schmitt, P., & Simmons, J. E. 1998, *Proc. SPIE*, 3354, 810
- Hinkle, K. H., Fekel, F. C., Johnson, D. S., & Scharlach, W. W. G. 1993, *AJ*, **105**, 1074
- Hinkle, K. H., Fekel, F. C., Joyce, R. R., Wood, P. R., Smith, V., & Lebzelter, T. 2006, *AJ*, **641**, 479
- Hinkle, K. H., Lebzelter, T., Joyce, R. R., & Fekel, F. C. 2002, *AJ*, **123**, 1002
- Hoard, D. W. 1993, *PASP*, 105, 1232
- Houk, N. 1963, *AJ*, **68**, 253
- Hughes, S. M. G., & Wood, P. R. 1990, *AJ*, **99**, 784
- Hut, P. 1981, *A&A*, **99**, 126
- Iben, I., Jr. 2003, in ASP Conf. Ser. 303, *Symbiotic Stars Probing Stellar Evolution*, ed. R. L. M. Corradi, J. Mikołajewska, & T. J. Mahoney (San Francisco, CA: ASP), 177
- Iben, I., Jr., & Tutukov, A. V. 1996, *ApJS*, **105**, 145
- Joyce, R. R. 1992, in ASP Conf. Ser. 23, *Astronomical CCD Observing and Reduction Techniques*, ed. S. Howell (San Francisco, CA: ASP), 258
- Joyce, R. R., Hinkle, K. H., Meyer, M. R., & Skrutskie, M. F. 1998, *Proc. SPIE*, 3354, 741
- Kalirai, J. S., Hansen, B. M. S., Kelson, D. D., Reitzel, D. B., Rich, R. M., & Richer, H. B. 2008, *ApJ*, **676**, 594
- Karovska, M., Carilli, C. L., Ramond, J. C., & Mattei, J. A. 2007, *ApJ*, **661**, 1048
- Kenyon, S. J., & Fernandez-Castro, T. 1987, *AJ*, **93**, 938
- Kenyon, S. J., Fernandez-Castro, T., & Stencel, R. E. 1988, *AJ*, **95**, 1817
- Kiss, L. L., Szatmáry, K., Szabó, G., & Mattei, J. A. 2000, *A&AS*, **145**, 283
- Kotnik-Karuzza, D., Jurkic, T., & Friedjung, M. 2007, *Baltic Astron.*, **16**, 98
- Lebzelter, T., Kiss, L. L., & Hinkle, K. H. 2000, *A&A*, **361**, 167
- Liebert, J., Bergeron, P., Eisenstein, D., Harris, H. C., Kleinman, S. J., Nitta, A., & Krzesinski, J. 2004, *ApJ*, **606**, L147
- Lu, W., & Rucinski, S. M. 1999, *AJ*, **118**, 515
- Luna, G. J. M., & Sokolowski, J. L. 2007, *ApJ*, **671**, 741
- Mikołajewska, J., Selvelli, P. L., & Hack, M. 1988, *A&A*, **198**, 150
- Mikołajewski, M., Mikołajewska, J., & Khudiakova, T. N. 1990, *A&A*, **235**, 219
- Mikołajewski, M., Mikołajewska, J., & Khudyakova, T. N. 1992, *A&A*, **254**, 127
- Mikołajewski, M., Mikołajewska, J., Tomov, T., Kulesza, B., Szczerba, R., & Wikierski, B. 1990, *Acta Astron.*, **40**, 129
- Mikołajewski, M., Tomov, T., & Mikołajewska, J. 1987, *Ap&SS*, **131**, 733
- Mikkola, S., & Tanikawa, K. 1998, *AJ*, **116**, 444
- Muciek, M., & Mikołajewski, M. 1989, *Acta Astron.*, **39**, 165
- Munari, U., Yudin, B. F., Kolotilov, E. A., & Tomov, T. V. 1996, *A&A*, **311**, 484
- Mürset, U., Dumm, T., Isenegger, S., Nussbaumer, H., Schild, H., Schmid, H. M., & Schmutz, W. 2000, *A&A*, **353**, 952
- Mürset, U., Nussbaumer, H., Schmid, H. M., & Vogel, M. 1991, *A&A*, **248**, 458
- Muterspaugh, M. W., et al. 2008, *AJ*, **135**, 766
- Nussbaumer, H., & Vogel, M. 1996, *A&A*, **307**, 470
- Olivier, E. A., & Wood, P. R. 2003, *ApJ*, **584**, 1035
- Payne-Gaposkin, C. 1954, *Ann. Harvard College Observatory*, **113**, 189
- Percy, J. R., Bakos, A. G., Besla, G., Hou, D., Velocci, V., & Henry, G. W. 2004, in ASP Conf. Ser. 310, *Variable Stars in the Local Group*, ed. D. W. Kurtz & K. R. Pollard (San Francisco, CA: ASP), 348
- Podsiadlowski, Ph., & Mohamed, S. 2007, *Baltic Astronomy*, **16**, 26
- Prieur, J. L., Aristidi, E., Lopez, B., Scardia, M., Mignard, F., & Carbillet, M. 2002, *ApJS*, **139**, 249
- Richichi, A., Fabbroni, L., Ragland, S., & Scholz, M. 1999, *A&A*, **344**, 511
- Rodgers, B., Hoard, D. W., Burdullis, T., Machado Pelaez, L., O'Toole, M., & Reed, S. 1997, *PASP*, **109**, 1093
- Russell, H. N., Dugan, R. S., & Stewart, J. Q. 1955, *Astronomy II – Astrophysics & Stellar Astronomy* (Boston, MA: Ginn), 700
- Scarfe, C. D., Batten, A. H., & Fletcher, J. M. 1990, *Publ. Dominion Astrophys. Obs. Victoria*, **18**, 21
- Schild, H., Dumm, T., Folini, D., Nussbaumer, H., & Schmutz, W. 1999, ed. P. Cox & M. F. Kessler *The Universe as Seen by ISO (ESA-SP 427; ESA, Noordwijk)*, 397
- Schmidt, M. R., Začs, L., Mikołajewska, J., & Hinkle, K. H. 2006, *A&A*, **446**, 603
- Schmutz, W., Schild, H., Mürset, U., & Schmid, H. M. 1994, *A&A*, **288**, 819
- Skopal, A. 1995, *IBVS*, 4157
- Skopal, A. 1997, in *Physical Processes in Symbiotic Binaries and Related Systems*, ed. J. Mikołajewska (Warsaw: Copernicus Foundation for Polish Astronomy), 99
- Skopal, A. 1998, *A&A*, **338**, 599
- Skopal, A., Bode, M. F., Lloyd, H. M., & Tamura, S. 1996a, *A&A*, **308**, L9
- Skopal, A., Vaňko, M., Pribulla, T., Chochol, D., Semkov, E., Wolf, M., & Jones, A. 2007, *Astron. Nachr.*, **328**, 909
- Skopal, A., et al. 1996b, *MNRAS*, **282**, 327
- Soker, N. 2000, *A&A*, **357**, 557
- Sokolowski, J. L., & Kenyon, S. J. 2003a, *ApJ*, **584**, 1021
- Sokolowski, J. L., & Kenyon, S. J. 2003b, *ApJ*, **584**, 1027
- Solf, J. 1987, *A&A*, **180**, 207
- Soszyński, I. 2007, *ApJ*, **660**, 1486
- Soszyński, I., et al. 2004, *Acta*, **54**, 347
- Soszyński, I., et al. 2007, *Acta*, **57**, 201
- Szewczyk, O., et al. 2008, *AJ*, **136**, 272
- Taranova, O. G., & Shenavrin, V. I. 2004, *Astronomy Reports*, **48**, 813
- Taranova, O. G., & Shenavrin, V. I. 2007, *Astronomy Letters*, **33**, 531
- Taylor, A. R., Seaquist, E. R., & Mattei, J. A. 1986, *Nature*, **319**, 38
- Unno, W., Osaki, Y., Ando, H., Saio, H., & Shibahashi, H. 1989, *Nonradial Oscillations of Stars* (Tokyo: Univ. Tokyo Press), 32
- van Leeuwen, F. 2007, *Hipparcos, the New Reduction of the Raw Data* (Heidelberg: Springer)
- Vassiliadis, E., & Wood, P. R. 1993, *ApJ*, **413**, 641
- Viotti, R., Badiali, M., Cardini, D., Emanuele, A., & Iijima, T. 1997, in *Hipparcos Venice '97*, ed. B. Battrock, *ESA, SP-402*, 405
- Walder, R., Folini, D., & Shore, S. N. 2008, *A&A*, **484**, L9
- Warner, B. 1972, *MNRAS*, **159**, 95
- Webster, B. L., & Allen, D. A. 1975, *MNRAS*, **171**, 171
- Whitelock, P. A. 1987, *PASP*, **99**, 573
- Wolff, C. L. 1996, *ApJ*, **459**, L103
- Wood, P. R. 2007, in ASP Conf. Series 362, *7th Pacific Rim Conference on Stellar Astrophysics*, ed. Y. W. Kang, H. W. Lee, K. S. Chen, & K. C. Leung (San Francisco, CA: ASP), 234
- Wood, P. R., Olivier, E. A., & Kawaler, S. D. 2004, *ApJ*, **604**, 800
- Wood, P. R., & Sebo, K. M. 1996, *MNRAS*, **282**, 958
- Wood, P. R., & Zarro, D. M. 1981, *ApJ*, **247**, 247
- Wood, P. R., et al. 1999, in *IAU Symp. 191, Asymptotic Giant Branch Stars*, ed. T. Le Bertre, A. Lebre, & C. Waelkens (Dordrecht: Kluwer), 151
- Yamashita, Y., & Maehara, H. 1979, *PASJ*, **31**, 307
- Yoo, K. H., & Yamashita, Y. 1991, *Publ. Natl. Astron. Obs. Japan*, **2**, 1
- Zamanov, R. K., Bode, M. F., Melo, C. H. F., Bachev, R., Gomboc, A., Stateva, I. K., Porter, J. M., & Pritchard, J. 2007, *MNRAS*, **380**, 1053